ORIGINAL ARTICLE

Simplified Computational Fluid Dynamics Model for Perforated Mitral Valve

Rudiyanto Philman Jong [1,2], Nuraisyah Amira Mohd Daman Huri[3], Kahar Osman[1,4], Mohamad Ikhwan Kori[3]

[1] Faculty of Mechanical Engineering, Universiti Teknologi Malaysia, 81310 UTM Johor Bahru, Johor, Malaysia
[2] Department of Mechanical and Manufacturing Engineering, Faculty of Engineering, Universiti Malaysia Sarawak, 94300 Kota Samarahan, Sarawak, Malaysia
[3] Department of Biomedical Engineering and Health Sciences, Faculty of Electrical Engineering, Universiti Teknologi Malaysia, 81310 UTM Johor Bahru, Johor, Malaysia
[4] IJN-UTM Cardiovascular Engineering Center, Universiti Teknologi Malaysia, 81310 UTM Johor Bahru, Johor, Malaysia

ABSTRACT

Introduction: Functional mitral regurgitation (Type I) could occur due to leaflet perforation or cleft. There are risks of functional mitral regurgitation might worsen to degenerative regurgitation and ultimately mitral valve failure. Computational fluid dynamics (CFD), an in-silico method, is proven to have the capability of modeling blood flow in cardiovascular system, particularly in this case for regurgitation flow behaviour. **Materials and Methods**: This paper presented the application of computational fluid dynamics to evaluate the mitral regurgitation due to mitral valve leaflet perforation by simulating the hypertensive conditions and mitral valve perforation severities. **Results:** The results show that the amount of blood flow to the left atrium increased with the increased perforation severity and hypertension severity. The increase of perforation severity has caused the average reduction of blood flow percentage of up to approximately 8.01% for severe perforation.**Conclusion:** Hence, the more severe the hypertension and perforation, the more complications a person may experience. With more blood flow back to the left atrium, it may lead to several complications including hypoxemia and cyanosis.
Malaysian Journal of Medicine and Health Sciences (2025) 21(SUPP11):170-176.doi:10.47836/mjmhs.21.s11.24

Keywords: Simplified mitral valve, mitral regurgitation, mitral valve perforation, computational fluid dynamics, biofluid dynamics

Corresponding Author:
Mohamad Ikhwan Kori, PhD
Email: mohamadikhwan@utm.my
Tel: +60175018070

INTRODUCTION

The global burden of mitral regurgitation has been increasing worldwide (1) indicating that mitral regurgitation is still a major concern in medicine. There are two major categories related to mitral regurgitation (2); a) degenerative mitral regurgitation, where the mitral valve is defective, and b) functional mitral regurgitation, where the mitral valve is normal, both categories are not less important than the other (3). Degenerative mitral regurgitation, however, is clearly related to the failure of the mitral valve structure itself (4) and significant to the assessment of the mitral valve failure progression.

Previously, degenerative heart valve disease affected about 18.1 million people globally with estimated 0.2% mortality due to the disease (5). While sudden death due to valvular heart disease in native valves ranges between 1% to 5% on yearly basis (6). Degenerative heart valve disease has been defined on a wide context depending on the valve types and specific point of view of various authors (7). In general, the definition of degenerative heart valve often includes the symptoms of valve dysfunctions mainly stenosis and regurgitation.

Mitral regurgitation severities are classified in four types of Carpentier classifications; Type I, Type II, Type IIIa and Type IIIb (8) with Type I being the least severe and Type III as the most severe occurrence of regurgitation. Major classification on mitral regurgitation conditions is also referred as primary (degenerative) regurgitation and secondary (functional) (9) regurgitation which indicate the need for valve repair or replacement based on the

current stage of the regurgitation.

Functional mitral regurgitation (Type I) could occur due to leaflet perforation or cleft (10). There are risks of functional mitral regurgitation might worsen to degenerative regurgitation and ultimately mitral valve failure (2). While having a risk assessment model for mitral valve failure has been long desired by medical practitioners (11), the development of assessment model for risk mitral valve failure is still not readily available (12). This has left the medical practitioners to rely mostly on their observation and experiences for their decision making on the patients' treatment (13).

Computational fluid dynamics (CFD), an in-silico method, is proven to have the capability of modeling blood flow in cardiovascular system (14), particularly in this case for regurgitation flow behaviour (15). Therefore, this provides an insight on the effect of different perforation size with different peak systolic pressure to the regugitation severity. Through an analysis of the effects of particular parameters on blood flow, such as peak systolic pressure and perforation size, this paper is hopefully will provide an opening to an option for non-invasive technique on visualizing the mitral valve while giving insight on the pathophysiology of the disease.

MATERIALS AND METHODS

Simplified mitral valve geometry

Simplified mitral valve geometry was created with a commercial CAD software to represent healthy and perforated mitral valve leaflet. A one side of bileaflet valve that mimics the shape of mitral valve was created with thickness of 3 mm (16) and length from anterior and posterior annular midpoints to coaptation of 20 mm and 15 mm respectively as shown in Figure 1 (a) (17). Figure 1 (b) shows the top view of the mitral valve model, with semi-lunar shape for each of the mitral valve leaflet.

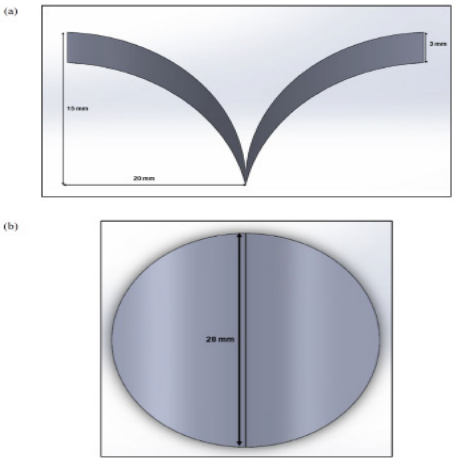

Figure 1: Simulation model and mesh generation

Flow channel for simulation

Enclosure or flow channel is a requirement for flow simulation with computational fluid dynamics, Therefore, simplified left ventricle, left atrium and aorta model was created for the enclosure of the mitral valve to represent the position of mitral valve in between of the left ventricle and left atrium. Left ventricle and aorta was created with the radius of 12 mm (18) and 10 mm (19) respectively. The aortic valve was excluded in this model as the aortic valve will remain fully open during peak systole to allow blood flow from the left ventricle. This condition mimics the scenario of fully closed mitral valve at peak systole when the pressure differential between left ventricle and left atrium is at the highest. Hence, the purpose of this simplified simulation model to reduce to the most critical scenario of mitral regurgitation which is a criteria for regurgitation severity assessment (20). This study evaluate the mitral regurgitation condition at mitral valve closure during peak systole only. Therefore, steady state simulation is sufficient to represent the scenario. Figure 2(a) shows the details of the flow channel and Figure 2(b) shows the position of the mitral valve in the flow channel.

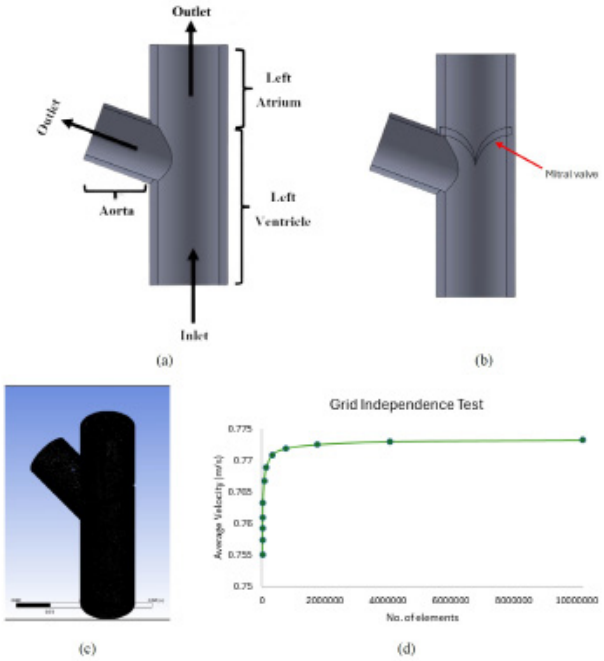

Figure 2: Simplified mitral valve geometry for simulation

Mitral valve leaflet perforation

Perforated mitral valve was represented by the area of holes on the mitral valve leaflet. The effect of perforation size to the regurgitation severity was simulated based on the size of perforated area. The size of perforation was varied to simulate the perforation severity that was expected to affect the severity of mitral regurgitation as well. The perforation sizes that represent different perforation severities were determined based on the previous study by (21). Perforation sizes based on mitral regurgitation severity were 10 mm^2 for mild, 20 mm^2 for moderate and 40 mm^2 for severe. The simplified

peforation is modeled as circular perforations (holes) based on the specified sizes of cross sectional area imposed on the mitral valve leaflet. Similar simulations setup for all perforated mitral valve models to simulate the flow behaviour of mitral regurgitation at mitral valve closure.

Governing equations

Accurate simulation and analysis of fluid flow with computational fluid dynamics require an understanding on the governing parameters and behaviors. The Navier-Stokes energy equations is the basis of this understanding, which efficiently model and predict flow dynamics across diverse fluid systems (22).

Fluid dynamics within the left ventricle are modeled using the incompressible Navier-Stokes equations, relating the velocity field and pressure field, with the blood that is assumed as Newtonian fluid with density, ρ and viscosity, μ within a defined region (23). The analysis are governed by the following continuity and Navier-Stokes Equations (1) and (2):

$$\nabla \cdot V = 0 \quad (1)$$

$$\frac{\delta v}{\delta t} + V \cdot \nabla V = -\nabla p + \mu \nabla^2 V \quad (2)$$

where V is the velocity, p is the pressure field and μ is the dynamic viscosity of blood.

The governing equations is solved by finite volume method within the comercially available ANSYS Fluent. Convergence criteria for the solution was set at 1×10^{-3} for the absolute value of the residual parameters or up to 1000 iterations. All simulations converged in less than 1000 interations.

Mesh of computational domain

Mesh was generated by ANSYS meshing with specific tune to ANSYS Fluent. Grid independence test was performed to find the optimum mesh configuration. Tetrahedral mesh was selected with optimum mesh elements of at 3×10^{-4} mm based on the results of grid independence test as in Figure 2(d). Figure 2(c) shows a sample of generated computation mesh for the simulation. Number of elements for the optimized mesh was at around 4×10^{6} elements.

Properties and boundary conditions

The simulation was perfomed with k-epsilon turbulent model in ANSYS Fluent. K-epsilon model was selected due to the focus of this study that is on the overall flow behavior instead of the near wall flow behavior (24). Distinct materials were assigned to represent both healthy and perforated valve conditions which can accurately predict flow characteristics within the fluid domain, enabling the analysis of flow rate effects for each state. The fluid type was assigned as blood with density of 1060 kg/m3 and dynamic viscosity of 0.0035 Pa.s (25). While non-Newtonian effects exist in all fluids, the influence of it diminishes in scenarios with large diameters and steady flow (26). So, Newtonian behavior was safely assumed. Blood was also assumed to be incompressible to maintain the fluid density (26). The simulation was set to be steady flow simulation to evaluate the flow characteristics at peak systolic. Inlet and outlets that are defined as the boundary condition of the model are shown in Figure 2(a). The inlet boundary was set at left ventricle while the outlets were set to be the left atrium and the aorta.

(27) specify the velocity of blood flow through the aorta at peak systolic at different hypertension level which were no hypertension, at risk of hypertension and hypertension. According to the conservation of mass, the flow rate of inlet is equal to the flow rate of outlet as in Equation (3). The velocity of blood at inlet are calculated using Equation (4).

$$Q_{Inlet} = Q_{Outlet} \quad (3)$$

$$V_{Inlet} A_{Inlet} = V_{Outlet} A_{Outlet} \quad (4)$$

where Q is the volumetric flow rate, V is the velocity and A is the cross sectional area. Thus, velocity of blood flowing through left ventricle can be calculated and used as the inlet boundary for steady state simulation. Peak systolic pressures were set to 122.5 mmHg for No Hypertension, 135 mmHg for At Risk and 157.5 mmHg for Hypertension. Inlet velocity at the left ventricle for No Hypertension, At Risk and Hypertension were set to 0.077083 m/s, 0.79861 m/s and 0.82639 m/s respectively. The pressure was set at 0 Pa of gauge pressure with reference to atmospheric pressure for both atrium and ventricle outlets in the simulation model (28). This is a simplified estimation to create common pressure differential across the inlet and outlet of the simulation model.

Evaluation of flow behaviour

The flow rate of blood through the mitral valve is considered with the condition of flow rate of inlet is equal to the flow rate of outlet as in Equation (3), based on conservation of mass. Thus, the total flow rate of blood from left ventricle is equal to the total of blood flow through the aorta and left atrium as in Equation (5).

$$Q_{LeftVentricle} = Q_{Aorta} + Q_{LeftAtrium} \quad (5)$$

where $Q_{LeftVentricle}$ is the flow rate of blood from left ventricle, Q_{Aorta} is the flow rate of blood to the aorta, and $Q_{LeftAtrium}$ is the flow rate of blood to the left atrium.

The total flow rate of blood through the mitral valve can be calculated using total flow rate of blood to the left

atrium as in Equation (6). Flow rate of blood flow to the left atrium is equal to the product of velocity of blood through mitral valve and the area of perforation of mitral valve as in Equation (7).

$$Q_{LefAtrium} = Q_{Valve} \quad (6)$$

$$Q_{LefAtrium} = V_{Valve} A_{Valve} \quad (7)$$

Where Q_{Valve} is the flow rate of blood through the mitral valve, V_{Valve} is the velocity of blood through the mitral valve, and A_{Valve} is the area of perforation size on mitral valve. To analyse the effect of pressure difference to the regurgitation severity, pressure difference between left ventricle and left atrium is calculated by using Equation (8).

$$\Delta P = P_{LV} - P_{LA} \quad (8)$$

where P_{LV} is the pressure of the left ventricle, P_{LA} is the pressure of the left atrium and ΔP is the pressure difference between left ventricle and left atrium.

The percentage of blood flow reduction to the aorta can be calculated by the ratio between velocity of blood flow to the left atrium and velocity of blood flow from left ventricle is calculated using Equation (9).

$$PR\% = \frac{V_{LA}}{V_{LV}} .100\% \quad (9)$$

here PR% is the percentage of reduction of blood flow to the aorta, V_{LA} is the velocity of blood to the left atrium, and V_{LV} is the velocity of blood from the left ventricle.

RESULTS

Behavior of Blood Flow due to Hypertension Severity

Figure 3 shows the distribution of the blood flow at different perforation severities with different hypertension severities. The red streaks indicate the highest velocity of blood flow. It differs with each model due to the different initial blood velocity set to mimic different stages of hypertension. For example, blood velocity to the aorta for mitral valve without perforation recorded the values of 1.145 m/s, 1.185 m/s and 1.235 m/s for No Hypertension, At Risk and Hypertension conditions. The outlet velocity of blood flow increases with the inlet velocity of blood flow. Thus, person with hypertension have the highest velocity of blood flow out of left ventricle.

At mild perforated mitral valve, there are blood flow back to the left atrium. However, due to the small size of perforation, the velocity of blood flow back to the left atrium is small compared to the moderate and severe perforated valve. Due to the nature of the simulation that was performed with steady state condition, the accumulation of flow at the left atrium seems to be significant. However, if the flow is considered as an instantenous flow, the amount of blood flow at the perforation opening was considerable low. But with the increase of systolic pressure due to hypertension, the regurgitation flow amount might significantly increased, hence reducing the cardiac output.

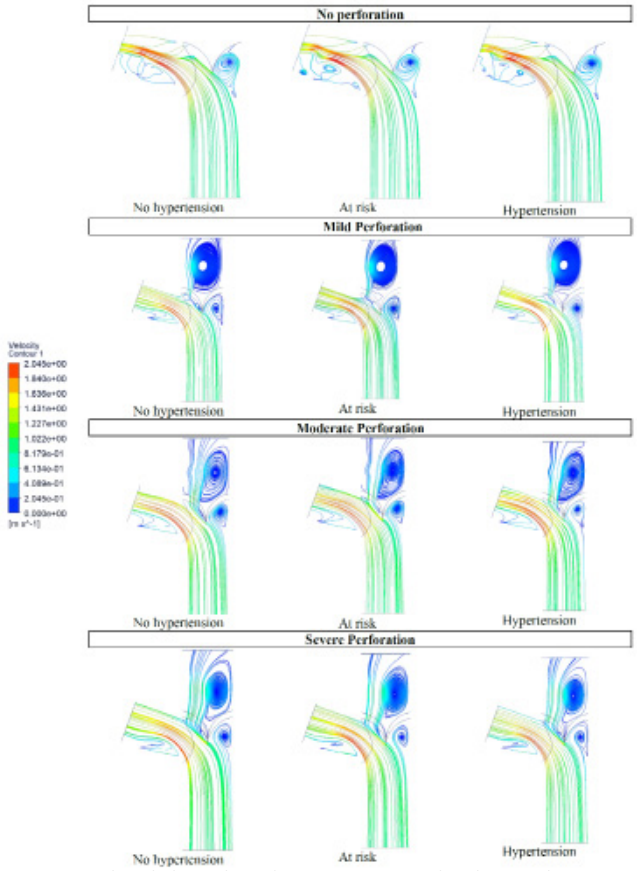

Figure 3: Blood flow distribution for mitral valve at different perforation severities

Figure 4 illustrates the velocity of blood flow through the perforated mitral valves across varying hypertension severities (No Hypertension, At Risk, Hypertension) and perforation severities (Mild, Moderate, Severe). Blood flow velocity increases with both the severity of hypertension and mitral valve perforation. The highest velocity of 2.365 m/s is recorded in the severely perforated valve under hypertensive conditions. On the other hand, the lowest velocity of 0.133 m/s is recorded in the mildly perforated valve with hypertension. These findings provide relationships between hypertension and mitral valve perforation in determining blood flow dynamics, with implications for cardiac function and potential clinical outcomes.

Effects of Pressure Difference to the Regurgitation Severity

The pressure difference between left ventricle and left atrium can be calculated using Equation (6). Left atrial flow rate increases from 0.730 L/min in no hypertension condition to 0.881 L/min with hypertension condition, with ΔP rise from 5.452 mmHg to 6.184 mmHg

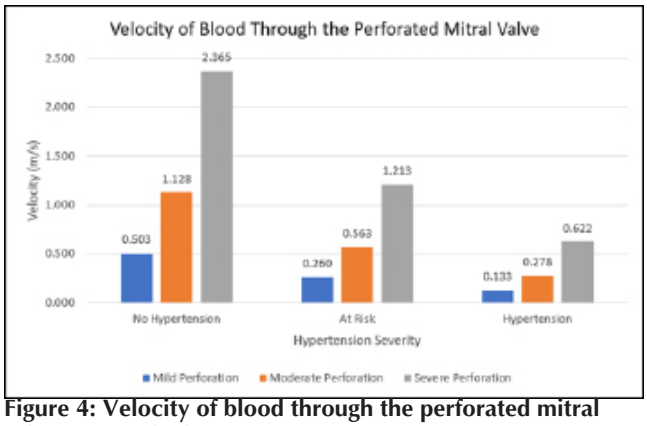

Figure 4: Velocity of blood through the perforated mitral valve against the hypertension severity

respectively. A similar pattern is observed in moderate regurgitation, where flow rate increases from 1.005 L/min to 1.084 L/min, and ΔP increases from 5.269 mmHg to 6.075 mmHg. Highest regurgitation flow rates were recorded in severe regurgitation condition, with left atrial flow rates increasing from 1.687 L/min in normotensive patients to 1.77 L/min in hypertensive patients. However, the ΔP in severe regurgitation shows a slight decrease from 4.515 mmHg to 5.090 mmHg, possibly due to reduced resistance to flow. These results represent hemodynamic burden imposed by the combination of regurgitation and hypertension, highlighting the potential for significant left atrial volume overload and increased ventricular afterload, particularly in severe regurgitation condition.

Regurgitation flow is evaluated based on the plot in Figure 5. Severe perforation records the smallest pressure difference between left ventricle and left atrium with the highest flow rate of blood to the left atrium compared

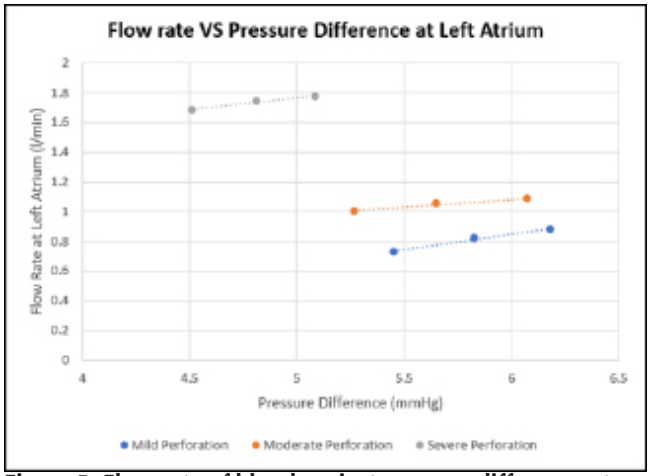

Figure 5: Flow rate of blood against pressure difference at left atrium

to mild perforation which has the lowest flow rate of blood to the left atrium but larger pressure difference between left ventricle and left atrium. However, mild perforation and moderate perforation has almost the same value of flow rate and pressure difference between left ventricle and left atrium which may resulted from the perforation size of both severity where mild perforation area and moderate perforation area is 10 mm^2 and 20 mm^2 respectively with only 10 mm^2 of difference. Thus, it explains the close values for both perforation severity. A direct correlation exists between perforation severity and both regurgitant flow and pressure difference, where severe perforated valve has the highest flow rate at low pressure difference.

Figure 6 shows the average percentage of reduction of blood flow rate to the aorta. With the increased of perforation severity, the average reduction of blood flow percentage increased up to approximately 3.73% for mild perforation, 4.83% for moderate perforation and 8.01% for severe perforation. This indicates that when perforation severity increased, the average percentage of reduction of blood to the aorta also increased, making less blood will flow to the aorta which may lead to less oxygenated blood flowing to the systemic circulation. This may lead to several complications including hypoxemia and cyanosis (29). However, at moderate perforation and severe perforation, the percentage of reduction decreased at hypertension. This is due to the velocity from the left ventricle and velocity of blood at the left atrium has little significance difference making the percentage of reduction lower than the one at at risk of hypertension.

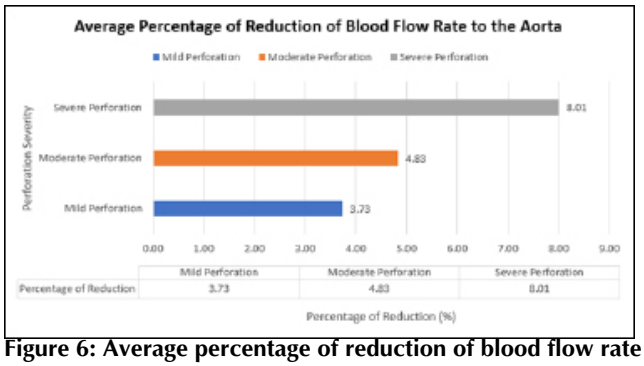

Figure 6: Average percentage of reduction of blood flow rate to the aorta

DISCUSSION

In the healthy mitral valve model, all blood from the left ventricle were delivered to the aorta as the mitral valve was performing well to prevent backflow of blood during peak systolic. As for defected mitral valve model (perforated mitral valve), most of the blood were delivered to the aorta. However, there were presence of blood backflow (regurgitation) to the left atrium due to the perforation in the mitral valve model.

Mitral valve perforation with hypertension records the highest velocity of blood flow to the left atrium due to high velocity (caused by high blood pressure) at the left ventricle inlet. When in combination with the severe perforation, hypertension condition worsen the regurgitation severity. This is due to the combination of high pressure and large orifice area for the regurgitation flow to take place. However, the bigger the size of perforation, does not contribute to the increased of the

velocity of blood passing through the perforation orifice. This is highly likely due to the increased cross sectional area would decrease the flow velocity but doesn't necessarily decreased the regurgitation volume.

In healthy mitral valve model, there is no presence of blood backflow (regurgitation) to the left atrium as the mitral valve is closed tightly, preventing regurgitation as expected. This allows fully functionality of blood delivery from left ventricle to the aorta. However, mitral regurgitation disrupts healthy mitral valve function, allowing backflow from the left ventricle to the left atrium during peak systole. This regurgitant volume elevates left atrium pressure which impacts the usual left ventricle filling. The elevated left atrium pressure increases left ventricle end-diastolic pressure and preload causing left ventricle to contracts more forcefully. However, the net forward stroke volume is ultimately lowered due to the left ventricle stroke volume bypassing the aorta and re-entering the left atrium (30).

According to a study by Rausch et al. (31), greater pressure differential between left ventricle and left atrium causes mitral valve to close tightly, restricting blood to backflow. From the results, pressure difference at severe perforation is the lowest followed by moderate perforation and mild perforation. As we compared the flow rate of blood to the left atrium as in Fig. 10, mild perforation records lower flow rate of blood to the left atrium compared to the moderate perforation and severe perforation which were represented by the velocity of blood flow to the left atrium and cross sectional area of the perforation. This justifies that higher pressure difference between left ventricle and left atrium makes it harder for blood to flow to the left atrium, thus restricts it from backflowing.

Recirculation of blood flow was presence at most of the simulated conditions mainly at the left atrium and left ventricle near the mitral valve. This flow behaviour most likely due to stagnation region at the left atrium and sudden drop of flow velocity from the left ventricle to the left atrium through the perforated mitral valve (32). As the valve is perfectly sealed due to the perforation, the recirculation zones are more obvious on perforated mitral valve as compared to normal mitral valve. This scenario is worth to be futher assessed on the wall shear stress imposed by the flow to the ventricle and atrial walls.

CONCLUSION

The flow rate of blood flow to the left atrium against the pressure difference between left ventricle and left atrium exhibits a nonlinear trend. Severe perforation shows smaller pressure difference between left ventricle and left atrium but at higher flow rate of blood to the left atrium compared to the other perforation severity.

The volume of blood that does not flow to the aorta is determined from the percentage of reduction of blood flow to the aorta. With the increase of perforation severity, the reduction of blood flow percentage increased up to approximately 3.73% in mild perforation, 4.83% in moderate perforation and 8.01% in severe perforation.

Through the computational fluid dynamics analysis of flow behaviour of blood through the different size of perforation at different severity of hypertension, this project can help identify patients who are more likely to experience complications. Early detection may prevent heart disease and other serious complications and allow more focused treatment. Personalised treatments for patients with perforated mitral valve may be developed by gaining an understanding on how flow behaviour of blood may be influenced by the severity of hypertension. This may involve in adjusting hypertension medication dosage or choosing the best time for surgery depending on a patient's own risk factors.

ACKNOWLEDGEMENTS

The authors would like to acknowledge the financial support from Universiti Teknologi Malaysia for the funding under UTM Encouragement Research Grant (UTMER) (Q.J130000.3823.31J13).

REFERENCE

1. Altes A, Vermes E, Levy F, Vancraeynest D, Pasquet A, Vincentelli A, et al. Quantification of primary mitral regurgitation by echocardiography: A practical appraisal. 2023;10.
2. La Canna G, Scarfo' I, Caso I. How to differentiate functional from degenerative mitral regurgitation. 2018;19:e75-e9.
3. Sideris K, Boehm J, Voss B, Guenther T, Lange RS, Guenzinger R. Functional and Degenerative Mitral Regurgitation: One Ring Fits All? Thorac Cardiovasc Surg. 2019;68(06):470-7.
4. Antoine C, Mantovani F, Benfari G, Mankad SV, Maalouf JF, Michelena HI, et al. Pathophysiology of Degenerative Mitral Regurgitation. 2018;11(1):e005971.
5. Yadgir S, Johnson CO, Aboyans V, Adebayo OM, Adedoyin RA, Afarideh M, et al. Global, Regional, and National Burden of Calcific Aortic Valve and Degenerative Mitral Valve Diseases, 1990–2017. 2020;141(21):1670-80.
6. Henriques de Gouveia R, Corte Real Gonɜalves FMA. Sudden cardiac death and valvular pathology. Forensic sciences research. 2019;4(3):280-6.
7. Dvir D, Bourguignon T, Otto CM, Hahn RT, Rosenhek R, Webb JG, et al. Standardized Definition of Structural Valve Degeneration for Surgical and Transcatheter Bioprosthetic Aortic Valves. 2018;137(4):388-99.
8. Topilsky Y. Mitral Regurgitation: Anatomy,

Physiology, and Pathophysiology—Lessons Learned From Surgery and Cardiac Imaging. 2020;7.
9. Iung B, Urena M. Transcatheter mitral valve repair for primary and secondary mitral regurgitation: new insights from a nationwide registry. 2021;23(8):1377-9.
10. Carpentier A. Cardiac valve surgery—the "French correction". The Journal of Thoracic and Cardiovascular Surgery. 1983;86(3):323-37.
11. Shen X, Wang T, Cao X, Cai L. The geometric model of the human mitral valve. PLOS ONE. 2017;12(8):e0183362.
12. Anbarasi A, Ravi S, Vaishnavi J, Matla SVSB. Computer aided decision support system for mitral valve diagnosis and classification using depthwise separable convolution neural network. Multimedia Tools and Applications. 2021;80(14):21409-24.
13. Mischa K, Roberto C, Georg N, Silke K, David H, Christophe W, et al. Heart team approach in treatment of mitral regurgitation: patient selection and outcome. Open Heart. 2020;7(2):e001280.
14. Dedи L, Menghini F, Quarteroni A. Computational fluid dynamics of blood flow in an idealized left human heart. 2021;37(11):e3287.
15. Lantz J, Bɑck S, Carlhɑll C-J, Bolger A, Persson A, Karlsson M, et al. Impact of prosthetic mitral valve orientation on the ventricular flow field: Comparison using patient-specific computational fluid dynamics. Journal of Biomechanics. 2021;116:110209.
16. Omran AS, Arifi AA, Mohamed AA. Echocardiography of the mitral valve. Journal of the Saudi Heart Association. 2010;22(3):165-70.
17. Oliveira D, Srinivasan J, Espino D, Buchan K, Dawson D, Shepherd D. Geometric description for the anatomy of the mitral valve: A review. 2020;237(2):209-24.
18. Olivotto I, Gistri R, Petrone P, Pedemonte E, Vargiu D, Cecchi F. Maximum left ventricular thickness and risk of sudden death in patients with hypertrophic cardiomyopathy. Journal of the American College of Cardiology. 2003;41(2):315-21.
19. Erbel R, Eggebrecht H. Aortic dimensions and the risk of dissection. Heart. 2006;92(1):137.
20. Grayburn PA, Thomas JD. Basic Principles of the Echocardiographic Evaluation of Mitral Regurgitation. 2021;14(4):843-53.
21. Brenneisen J, Wentzel C, Karwan F, Dussel O, Loewe A. Fluid dynamics in the human heart: Altered vortex formation and wash-out in mitral regurgitation simulations. 2021;7(2):199-202.
22. Tillman DA, Duong DNB, Harding NS. Chapter 7 - Modeling and Fuel Blending. In: Tillman DA, Duong DNB, Harding NS, editors. Solid Fuel Blending. Boston: Butterworth-Heinemann; 2012. p. 271-93.
23. Kronborg J, Svelander F, Eriksson-Lidbrink S, Lindstrum L, Homs-Pons C, Lucor D, et al. Computational Analysis of Flow Structures in Turbulent Ventricular Blood Flow Associated With Mitral Valve Intervention. 2022;Volume 13 - 2022.
24. Vostruha K, Pelant JJEWoC. Perturbation Analysis of "k—ω" and "k—ε" Turbulent Models. Wall Functions. 2013;45:01097.
25. Bennati L, Vergara C, Giambruno V, Fumagalli I, Corno AF, Quarteroni A, et al. An Image-Based Computational Fluid Dynamics Study of Mitral Regurgitation in Presence of Prolapse. Cardiovascular Engineering and Technology. 2023;14(3):457-75.
26. Al-Atabi M, Lim Y. Investigation of Blood Flow through the Mitral Valve. Journal of Engineering Science and Technology. 2014;Special Issue 8:68-78.
27. Li Y, Gu H, Fok H, Alastruey J, Chowienczyk P. Forward and Backward Pressure Waveform Morphology in Hypertension. Hypertension (Dallas, Tex : 1979). 2017;69(2):375-81.
28. Rahimi K, Mohseni H, Otto CM, Conrad N, Tran J, Nazarzadeh M, et al. Elevated blood pressure and risk of mitral regurgitation: A longitudinal cohort study of 5.5 million United Kingdom adults. PLOS Medicine. 2017;14(10):e1002404.
29. Lopaschuk GD, Jaswal JS. Hypoxia-Induced Adaptation to Mitral Regurgitation: A Role for KATP Channel Up-Regulation. Journal of the American College of Cardiology. 2012;59(4):397-9.
30. Gaasch WH, Meyer TE. Left Ventricular Response to Mitral Regurgitation. Circulation. 2008;118(22):2298-303.
31. Rausch MK, Famaey N, Shultz TOB, Bothe W, Miller DC, Kuhl E. Mechanics of the mitral valve. Biomechanics and Modeling in Mechanobiology. 2013;12(5):1053-71.
32. Rahma AG, Yousef K, Abdelhamid T. Blood flow CFD simulation on a cerebral artery of a stroke patient. SN Applied Sciences. 2022;4(10):261.